Journal of Magnetic Resonance 194 (2008) 163–168

Contents lists available at ScienceDirect

Journal of Magnetic Resonance

journal homepage: www.elsevier.com/locate/jmr

^{1}H NMR spectroscopy of rat brain *in vivo* at 14.1 Tesla: Improvements in quantification of the neurochemical profile

Vladimír Mlynárik *, Cristina Cudalbu, Lijing Xin, Rolf Gruetter

Laboratory of Functional and Metabolic Imaging (LIFMET), Ecole Polytechnique Fédérale de Lausanne, Station 6, CH-1015 Lausanne, Switzerland

ARTICLE INFO

Article history:
Received 21 February 2008
Revised 26 June 2008
Available online 28 June 2008

Keywords:
Proton single voxel spectroscopy
Ultra high magnetic field of 14.1 T
Rat brain
LCModel
Quantification accuracy

ABSTRACT

Ultra-short echo-time proton single voxel spectra of rat brain were obtained on a 14.1 T 26 cm horizontal bore system. At this field, the fitted linewidth in the brain tissue of adult rats was about 11 Hz. New, separated resonances ascribed to phosphocholine, glycerophosphocholine and *N*-acetylaspartate were detected for the first time *in vivo* in the spectral range of 4.2–4.4 ppm. Moreover, improved separation of the resonances of lactate, alanine, γ-aminobutyrate, glutamate and glutathione was observed. Metabolite concentrations were estimated by fitting *in vivo* spectra to a linear combination of simulated spectra of individual metabolites and a measured spectrum of macromolecules (LCModel). The calculated concentrations of metabolites were generally in excellent agreement with those obtained at 9.4 T. These initial results further indicated that increasing magnetic field strength to 14.1 T enhanced spectral resolution in ^{1}H NMR spectroscopy. This implies that the quantification of the neurochemical profile in rodent brain can be achieved with improved accuracy and precision.

1. Introduction

The ability of *in vivo* short echo-time ^{1}H NMR spectroscopy to determine the concentrations of at least 18 metabolites (the neurochemical profile) in rodent brain [1] opens the perspective of studying multiple biomarkers in rodent models of human diseases. Measurements at high magnetic fields are poised to benefit from the higher signal-to-noise ratio (SNR) and increased spectral dispersion, which likely improve quantification accuracy and precision. The benefits are especially expected to be important for metabolites having low concentration or overlapping spectral lines and for compounds giving complex *J*-coupled spectral patterns. Recent studies, however, have indicated that these advantages may be partially offset by a decrease of T_2 and T_2^* with increasing static magnetic field [2,3], with some predicting [4] a moderate increase of the signal-to-noise ratio (SNR) and a nearly linear increase in the spectral linewidth (expressed in Hz) when increasing B_0 above 9.4 T.

Most high-field short-echo *in vivo* proton spectroscopy measurements of rodents in the last decade have been performed at 9.4 T. It was shown that a combination of careful eddy current compensation [5], automatic first- and second-order localized shimming [6], and an ultra-short echo-time localization technique with efficient water suppression enabled to measure high quality spectra with resolved spectral lines of many metabolites (*e.g.*, the spectrally resolved signals of phosphocreatine and creatine at 3.9 ppm) [7]. The spectral resolution reported in proton spectra of rat brain at 11.7 T [8,9] appeared consistent with the aforementioned predictions [4].

Spectra measured at short echo-times are further complicated by broad signals ascribed mainly to cytosolic proteins [10]. At high magnetic fields the largely field-independent linewidth of the signals of macromolecules increasingly approaches that of metabolites and an experimental assessment of macromolecular contribution to the proton spectrum may become crucial for accurate metabolite quantification.

Even at the highest experimentally achievable magnetic field for *in vivo* experimentation, spectral overlap of proton signals from brain metabolites still may require that concentrations of metabolites are determined by fitting to the measured *in vivo* data a linear combination of a "basis set", *i.e.*, the spectra of individual metabolites (obtained either experimentally or using spin simulations [11]). The most frequently used programs for proton spectra quantification are JMRUI [12] and LCModel [13] working in the time and frequency domain, respectively. Provided such a basis set represents the tissue composition sufficiently well, the fitting routines are expected to be enough robust for the quantification of less abundant metabolites with spectral lines overlapped by dominant resonances. However, concentrations of metabolites, which are poorly characterized in the *in vivo* proton spectra, can be less accurate and their values can be substantially correlated with the concentrations of dominant metabolites. Thus, we expect that the

* Corresponding author. Fax: +41 21 6937960.
E-mail address: vladimir.mlynarik@epfl.ch (V. Mlynárik).

1090-7807/$ - see front matter © 2008 Elsevier Inc. All rights reserved.
doi:10.1016/j.jmr.2008.06.019

improved separation of spectral lines at higher magnetic fields results in a more accurate quantification.

With the availability of the first 14.1 T/26 cm MR system we aimed to implement and assess the performance of ultra-short echo-time proton localized spectroscopy of rat brain *in vivo* and to determine if new spectral features not previously reported at 9.4–11.7 T are present. More specifically, the obtained initial results were compared to the previously suggested field dependence of the spectral linewidth, together with an initial assessment of the reliability and accuracy of the calculated metabolite concentrations.

2. Methods

2.1. Animals

In vivo experiments were performed on the same group of male Sprague–Dawley rats, which were anesthetized with 1.5–2.5% isoflurane using a nose mask. All animal experiments were conducted according to federal and local ethical guidelines and the protocols were approved by the local regulatory body. Body temperature was maintained at 37.5 ± 1.0 °C by circulating warm water around the animals.

2.2. Instruments and pulse sequences

Proton spectra were measured from the brain of five animals using two MR instruments (Varian, Palo Alto, CA, USA): an INOVA spectrometer interfaced to a 9.4 T, actively shielded magnet with a 31-cm horizontal bore, and an MRI System interfaced to 14.1 T magnet with a 26-cm horizontal bore (both magnets from Magnex Scientific, Oxford, UK). The magnets were equipped with 12-cm inner-diameter actively shielded gradient sets (Magnex Scientific, Oxford, UK) allowing a maximum gradient of 400 mT/m in 120 μs. Home-built quadrature surface coils consisting of two geometrically decoupled 14-mm diameter single loops were used as both transmitter and receiver. The total width of the 9.4 T and 14.1 T RF coils was 18 mm and 21 mm, respectively. Eddy currents were minimized using time dependent quantitative eddy current field mapping [5]. The static field homogeneity was adjusted using first- and second-order shims using an EPI version of FASTMAP [14].

Localizer images were obtained in the coronal and horizontal planes using a multislice fast spin echo protocol with TE/TR = 60/5000 ms, a slice thickness of 1 mm and an isotropic in-plane resolution of 94 μm. Spectra were obtained by an ultra-short echo-time (TE/TR = 2.8/4000 ms) spin echo full intensity acquired localization (SPECIAL) technique [15], which combined 1D image-selected *in vivo* spectroscopy (ISIS) [16] in the vertical (*Y*) direction with a slice selective spin echo (SE) in the *X* and *Z* directions. The acquisition of 4096 complex points followed an add-subtract scheme as in 1D ISIS. Identical RF pulses, gradient amplitudes and sequence timing were used on both instruments. The spectral width was 5 kHz and 7 kHz at 9.4 T and 14.1 T, respectively. In the ISIS part of the sequence, a 2-ms slice selective full-passage hyperbolic secant adiabatic pulse with a bandwidth of 10 kHz was applied in alternate scans. In the SE part of sequence, a 0.5-ms 90° and a 1-ms 180° asymmetric slice-selective pulses [7,17] were used in the directions parallel to the coil plane. The bandwidths of the 90° and 180° pulses were 13.5 kHz and 5.8 kHz, respectively. VOIs of 50–70 μl were placed laterally to the brain midline and included frontal cortex, corpus callosum and striatum. The voxel position was identical at both field strengths.

Water signal was suppressed by a series of seven 25-ms asymmetric variable power RF pulses (bandwidth = 270 Hz) with optimized relaxation delays (VAPOR) [7]. The water suppression pulses were interleaved with three modules of outer volume saturation using six 1.2-ms full-passage hyperbolic secant band-selective pulses with a bandwidth of 35 kHz. Another frequency-selective saturation pulse (15 ms Gaussian, bandwidth = 180 Hz) was added in the delay between the ISIS and SE modules. For obtaining spectra with comparable SNR at both fields, the number of accumulations was varied from 64 to 160 at 9.4 T and from 16 to 160 at 14.1 T. Data processing included zero-filling up to 16 K data points, Gaussian weighting of the FID, Fourier transformation, and zero- and minimal first-order phase correction. To compensate for the magnetic field drift, spectra were collected in blocks of 16 averages, which were stored separately in the memory and were corrected for the relative shift in frequency.

For estimating the spectrum of macromolecules, the SPECIAL sequence was extended with a 2-ms nonselective full-passage hyperbolic secant inversion pulse (a bandwidth of 10 kHz), which was applied before starting the localization part of the sequence. The repetition time of 2500 ms and the echo time of 2.8 ms or 40 ms were used, the number of accumulations was 640. The macromolecule spectrum was discriminated from signals of metabolites based on a difference in T_1 relaxation times, which are much shorter in macromolecules also at 14.1 T. A series of short echo-time (TE = 2.8 ms) inversion recovery spectra were measured with inversion times (TI) of 420, 600, 750, 850 and 1000 ms.

2.3. Quantification

Metabolite concentrations were calculated by LCModel using databases of simulated spectra of metabolites combined with spectra of macromolecules measured at both fields. Databases of simulated spectra were created by a home written program in MATLAB (MathWorks, Natick, MA, USA) based on the density matrix formalism [18], using published values of coupling constants and chemical shifts [11]. The macromolecule spectrum at 14.1 T was measured as a part of this study while the spectrum for the 9.4 T database was taken from the previous study [15]. The spectrum of macromolecules at 14.1 T was processed using the Hankel–Lanczos singular value decomposition (HLSVD) technique [19] implemented in the JMRUI software. In order to assess the importance of the measured spectrum of macromolecules in the quantification of metabolites at 14.1 T, the LCModel analysis of a series of five spectra was repeated twice, with and without including the spectrum of macromolecules in the LCModel database, respectively. In the latter case, LCModel estimated the macromolecular "baseline" using predefined peaks of macromolecules and lipids and a spline function.

3. Results

A high magnet stability and the quality of the gradient system were considered important prerequisites for high performance of ^{1}H NMR spectroscopy. The magnetic field drift on the 14.1 T magnet was less than 0.05 ppm/hour. Eddy currents were minimized to below 0.02%. An increase of approximately 10–20% in SNR values provided by LCModel was observed at 14.1 T in comparison with 9.4 T. The best water and total creatine (CH_3) linewidths measured in 5 spectra of adult rats after FASTMAP optimization of first- and second-order shims were about 17 Hz and 14 Hz, respectively. The best values obtained at 9.4 T were about 12.5 Hz and 10.5 Hz for water and creatine signals, respectively.

3.1. New features of 14.1 T proton spectra

Fig. 1 shows single voxel 9.4 T and 14.1 T spectra of rat brain, measured by the SPECIAL technique, with peak assignments. Two

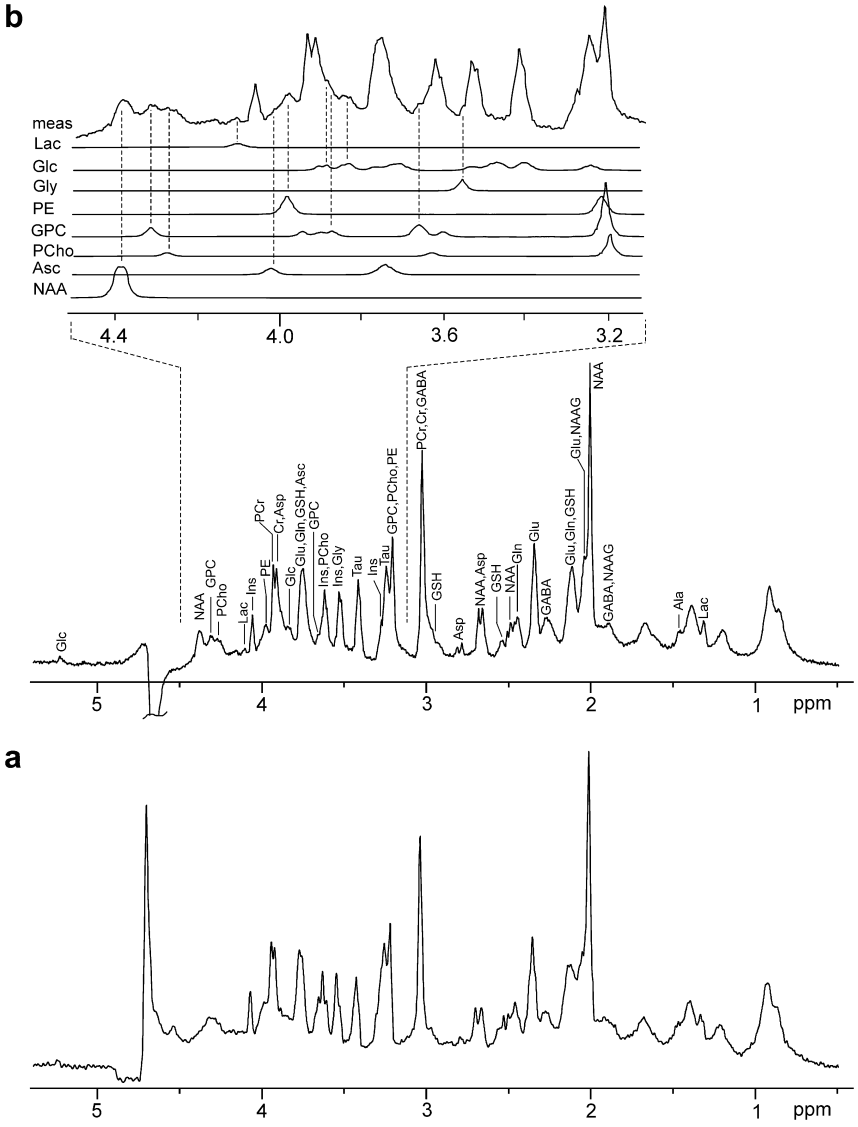

Fig. 1. Comparison of 9.4 T (a) and 14.1 T (b) spectra of rat brain. The expanded region of the 14.1 T spectrum shows the assignment of small peaks and peak shoulders in the downfield part of the spectrum to model spectra of individual metabolites. A shifted Gaussian function, $\exp[-(t-0.08)^2/0.11^2]$, was used in both spectra for modest resolution enhancement. The peak of NAA at 4.4 ppm in the 14.1 T spectrum is partially saturated by water suppression pulses.

novel prominent features were immediately apparent at 14.1 T, in particular a group of spectral lines resonating between 4.2 and 4.4 ppm, and the narrowing (in ppm) of the spectral lines of GABA, Glu and NAA in the spectral range from 1.8 ppm to 2.6 ppm. In the complex peak at 2.45–2.55 ppm, the glutamate CH_2 protons of GSH (2.56 ppm) were partially resolved from those of NAA (2.49 ppm).

This figure further illustrates increased dispersion at 14.1 T. The improved spectral quality enabled to discern several low-intensity peaks in the spectral region from 3.5 ppm to 4.2 ppm, which were assigned to Lac (at 4.11 ppm), Glc (3.85 ppm) and GPC (3.67 and 3.87 ppm) (Fig. 2, inset). The resonances in the chemical shift range above 4.2 ppm were detected for the first time *in vivo* due to the effectively narrower bandwidth used for water suppression, which represents a further manifestation of the increased spatial resolution. They were ascribed to NAA, GPC and PCho at 4.38, 4.31 and 4.27 ppm.

3.2. Estimation of the macromolecule spectrum at 14.1 T

The inversion recovery spectra measured with different inversion times are shown in Fig. 2. Residual peaks of major metabolites were seen in all the spectra due to the high SNR. Since T_1 relaxation times of metabolite resonances were not identical, a macromolecule spectrum with completely nulled metabolite resonances could not be obtained. Thus, the spectrum at TI = 750 ms (Fig. 2c) with the smallest, positive or negative, residual peaks was taken as a basis for the spectrum of macromolecules. Intensity of the residual metabolite peaks in this spectrum was less than 10% of the original signal intensity except for the Cr/PCr peak at 3.9 ppm having substantially shorter T_1 as in previous studies [1]. Identification of these peaks was based on the course of their intensities (changing from negative to positive) over the series of inversion recovery spectra. In addition, the identification was confirmed by measuring an inversion recovery spectrum with TI = 750 ms and TE = 40 ms (Fig. 2f). In this spectrum the residual signals of metabolites were retained due to longer T_2 relaxation times, while the signals of macromolecules were substantially reduced due to the more rapid signal decay, ascribed to faster T_2 relaxation. In this way, residual peaks of NAA at 2.0 and 2.7 ppm, Tau at 3.4 ppm, total choline at 3.2 ppm, Ins at 3.6 ppm and total Cr at 3.9 ppm were identified. The final macromolecule spectrum after removing residual peaks of metabolites is shown in Fig. 2g.

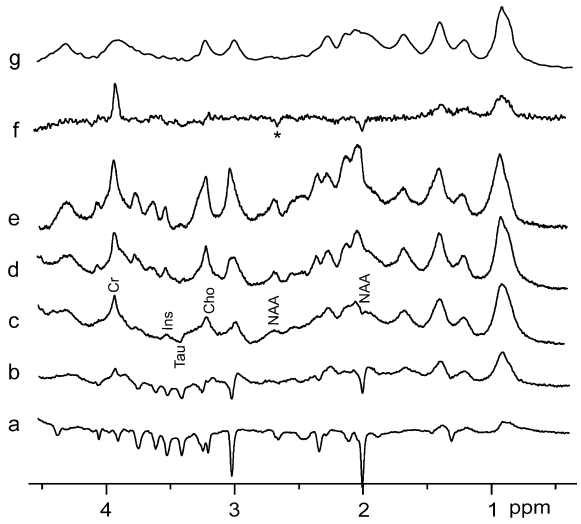

Fig. 2. Estimation of the spectrum of macromolecules based on IR-SPECIAL spectra using inversion times of 420 ms (a), 600 ms (b), 750 ms (c), 850 ms (d) and 1000 ms (e) and TE = 2.8 ms, and the spectrum measured with the inversion time of 750 ms and TE = 40 ms (f). The spectrum (c) showing minimal residual peaks (negative peaks of NAA at 2 ppm and Tau at 3.4 ppm, and positive peaks of NAA at 2.7 ppm, GPC/PCho at 3.2, Ins at 3.6 ppm and Cr/PCr at 3.9 ppm) was considered as a spectrum of macromolecules after removing the residual peaks of metabolites by the HLSVD algorithm (g). The residual signal of NAA at 2.7 ppm marked with asterisk in the spectrum (f) is reduced and inverted relative to that in the spectrum (c) due to J-evolution.

3.3. Determination of metabolite concentrations

Fig. 3 demonstrates that the spectrum fitted without an experimental macromolecule spectrum was a poorer match of the experimental spectrum, with residuals observed particularly in the spectral region from 0.5 to 2.0 ppm, compared to the LCModel run with the macromolecule spectrum. When omitting the spectrum of macromolecules, the metabolite concentrations of Glc, GABA, PCho, GSH, PE and Asp were higher by about 30–70% whereas the concentrations of Ala, Asc, NAAG and Lac were lower by 70–100% (data not shown).

The LCModel analysis of a representative 14.1 T spectrum is shown in Fig. 4. Five spectra having the same SNR (within ±3%) as judged from LCModel outputs at both fields were used to compare mean concentrations, their standard deviations and mean Cramer–Rao lower bounds (CRLB) for 19 metabolites (Table 1). The concentrations were fitted from the spectral ranges of either 0–4.1 ppm (at 9.4 T and 14.1 T) or 0–4.4 ppm (at 14.1 T only). In general, an excellent agreement between the concentrations obtained at 9.4 and 14.1 T was noted. Substantial differences were observed only for metabolites which are not well characterized at 9.4 T such as Ala, GPC and PCho, GABA, Gly and NAAG.

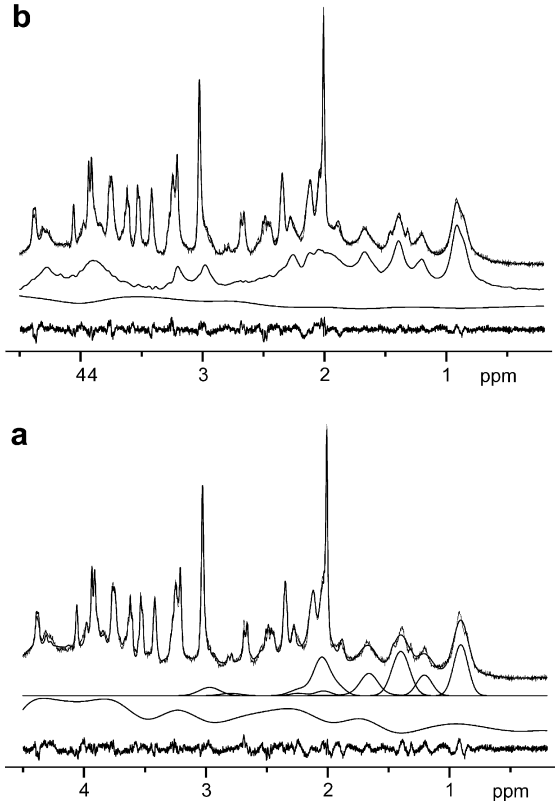

Fig. 3. Comparison of LCModel results obtained on the same spectrum using a spectral database without (a) and with (b) including the spectrum of macromolecules. The upper traces show overlaid experimental (thin line) and simulated (thick line) spectra. The traces below represent, from top to bottom, modeled (a) or experimental (b) macromolecules, residual baseline and the difference between the experimental and simulated spectra.

4. Discussion

A constant trend towards using higher magnetic fields is seen in high resolution NMR due to the increased SNR and improved resolution. However, the benefits of ultra high fields for *in vivo* MR spectroscopy may be offset by increases in linewidth due to the heterogeneity of the brain tissue.

Our experiments demonstrated new spectral features at 14.1 T not seen previously at 9.4–11.7 T. For example, the resolved resonances at 4.31 and 4.27 ppm, which typically are saturated at lower fields by water suppression pulses, and additional peaks/peak shoulders of GPC resolved between 3.6 ppm and 3.9 ppm (Fig. 1) may substantially improve the accuracy of the GPC and PCho quantification. The spectra of GPC and PCho at lower magnetic fields show only one common intense resonance line with almost identical chemical shifts, 3.212 ppm and 3.208 ppm, respectively [11]. The other small signals in the range of 3.6–3.9 ppm are obscured by intense signals of Ins, Glu, Gln, Cr and PCr, thus providing very few spectral features that can lead to a robust and separate quantification of GPC and PCho. The concentration of PCho calculated by LCModel at 9.4 T are larger than that of GPC, with calculated standard deviations of about 30%, whereas the concentrations obtained at 14.1 T are reversed and their standard deviations dropped by more than one-half (Table 1). The obtained concentrations of PCho and GPC can in principle be compared with ^{31}P NMR data, where PCho and GPC peaks have been resolved. We are aware only of studies on human brain [20] and on brain of newborn piglets [21] showing resolved PCho and GPC peaks. In these ^{31}P NMR spectra, peak intensities of GPC and PCho agree well with the GPC/PCho ratio found at 14.1 T. The importance of the upfield spectral region for the quantification of PCho and GPC is demonstrated by the LCModel fit at 14.1 T. When only the spectral range from 0 to 4.1 ppm was used (Table 1), standard deviations dramatically increased and the mean PCho and GPC concentrations changed. These data indicate that the detection of the new spectral lines at 14.1 T improves substantially the precision and likely also accuracy of quantification of GPC and PCho. Similarly, determination of Glc should be improved at 14.1 T since, along with the well-separated peak at 5.23 ppm, there is another spectral line of this compound at 3.85 ppm, which is clearly visible at 14.1 T even at euglycemia. However, the Glc and Lac concentrations could not be reliably compared with those at 9.4 T due to their dependence on animal physiology, such as anesthesia and glycemia.

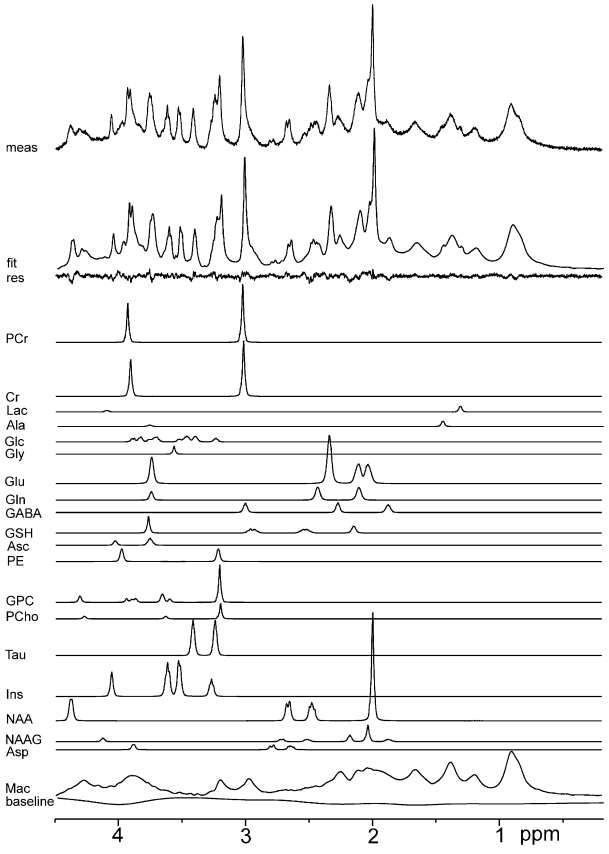

Fig. 4. From the top, a 14.1 T spectrum from rat brain (70 μl volume of interest including frontal cortex, corpus callosum and striatum, 240 scans), its LCModel fit and a residual spectrum. The spectra below are fits of individual metabolites. The symbols are explained in Table 1, Mac is the macromolecule spectrum.

Despite excellent spectral dispersion at 14.1 T, many spectral lines of metabolites remained overlapped among each other as well as with macromolecule signals. We demonstrated that an experimental estimation of the macromolecule spectrum representing the "baseline" of ultra-short echo-time proton spectra can improve the quality of the fit between experimental and simulated spectra at this magnetic field. The absence of the measured macromolecule spectrum in the database led to a large and unpredictable bias in concentrations of many metabolites, in the case of Lac even to the absence of any estimated value.

The estimated spectrum of macromolecule was obtained by a single inversion recovery technique, although this was not the only approach evaluated. The double inversion spectrum reproduced poorly our experimental "baseline" in the spectral region of 0.5–2 ppm because signal intensities in the macromolecule spectrum obtained by this method were differently T_1-weighted [4] (data not shown). Due to a relatively high SNR we were able to identify residual peaks of metabolites and remove them from the macromolecule spectrum in the time domain. The LCModel calculations, employing a database of simulated spectra of metabolites combined with the measured spectrum of macromolecules, provided an excellent fit to experimental data (Fig. 4).

Table 1 indicates that relative standard deviations and CRLBs of metabolite concentrations are nearly the same or lower at 14.1 T than at 9.4 T. It should be noted that spectra with the same SNR were compared. Therefore, the observed decrease of standard deviations of Ala, Asp, GABA, Gly and NAAG can be attributed to improved separation of their spectral lines. The removal of residual peaks from the spectrum of macromolecules at 14.1 T could further improve accuracy of quantification of some metabolites having

Table 1
Mean metabolite concentrations (±standard deviations) and mean CRLB calculated from five pairs of spectra measured at 9.4 T and 14.1 T, respectively

Metabolite	9.4 T		14.1 T	
	Concentration (mmol/kg) ± SD	CRLB (%)	Concentration (mmol/kg) ± SD	CRLB (%)
Alanine (Ala)	0.37 ± 40%	23	0.63 ± 19%[a]	11
Aspartate (Asp)	1.7 ± 31%	14	1.9 ± 10%	9
Phosphocholine (PCho)	0.47 ± 33%	16	0.32 ± 16%[a]	16
			0.49 ± 26%[b]	17
Glycerophosphocholine (GPC)	0.33 ± 30%	18	0.87 ± 5%[a]	6
			0.66 ± 32%[ab]	12
Creatine (Cr)	3.9 ± 12%	4	4.0 ± 11%	3
Phosphocreatine (PCr)	4.5 ± 9%	3	4.3 ± 10%	3
γ-Aminobutyrate (GABA)	1.1 ± 22%	9	1.5 ± 13%[a]	6
Glutamine (Gln)	3.0 ± 19%	3	2.8 ± 19%	3
Glutamate (Glu)	9.8 ± 6%	1.5	10.3 ± 8%	1.2
Glutathione (GSH)	1.0 ± 12%	7	1.3 ± 14%[a]	5
Glycine (Gly)	0.50 ± 32%	22	0.81 ± 17%	13
Glucose (Glc)	1.2 ± 66%	30	2.3 ± 10%[a]	9
myo-Inositol (Ins)	5.9 ± 6%	2	6.2 ± 5%	2
N-Acetylaspartate (NAA)	9.2 ± 10%	1.0	9.3 ± 12%	1.0
Taurine (Tau)	6.1 ± 12%	2	6.0 ± 9%	2
Ascorbate (Asc)	1.2 ± 40%	14	1.4 ± 33%	11
N-Acetylaspartylglutamate (NAAG)	0.40 ± 51%	6	0.96 ± 16%[a]	6
Phosphoethanolamine (PE)	2.1 ± 9%	6	2.2 ± 12%	9
Lactate (Lac)	1.4 ± 33%	7	0.73 ± 19%[a]	12

The spectra in each pair had the same SNR (within ±3%), the overall range of SNR was 27–40.

[a] Metabolite concentrations, which were found significantly different at 14.1 T compared to 9.4 T ($t < 0.1$).

[b] Only the spectral range from 0 to 4.1 ppm was used in the LCModel fit.

their spectral lines co-registered with the residual peaks, namely Gly, Asp and PCho. Thus, the concentrations of several poorly represented metabolites are expected to be more accurate at 14.1 T. Specifically, the Ala concentration of 0.6 mmol/kg found at 14.1 T is close to the value of about 0.65 mmol/kg found by *ex vivo* ^{1}H NMR in the rat cortex [22]. The concentration of GABA measured at 14.1 T is similar to the concentration of 1.8 mmol/kg found in the whole rat brain and to the average value of 1.25 and 2.21 mmol/kg found in rat cortex and striatum, respectively, by enzymatic–fluorometric analysis of brain extracts [23]. The LCModel estimate at 14.1 T for the Gly concentration was in excellent agreement with the value of 1.0 mmol/kg determined by high performance liquid chromatography in brain extracts [24] and by *in vivo* spectroscopy of rat brain at a longer echo time [25].

For comparing uncertainties of metabolite concentrations at both fields we used two parameters: standard deviations, which contain also inter-animal variations, and CRLBs. The CRLBs are estimates of standard deviations of concentrations in individual spectra, however, they assume that the model is correct or at least sufficiently parameterized to describe the data (S. Provencher, LCModel & LCMgui User's Manual, http://s-provencher.com/pages/lcmodel.shtml). Thus, comparison of CRLBs for PCho, GPC, Lac and NAA using different models, with and without spectral lines in the 4.1–4.4 ppm region, might not be fully adequate.

The smaller than the theoretically predicted 50% increase in sensitivity can be in part explained by small differences in hardware of both scanners. The width of the RF coil at 14.1 T was slightly larger than the width of the coil used at 9.4 T, which was estimated to account for a 25% decrease in signal intensity at 14.1 T. Another 10% signal attenuation was due to cable insertion losses at 14.1 T, which can be minimized by moving the preamplifier closer to the RF coil. Taking these differences in hardware into account, the observed increase in SNR at 14.1 T was consistent with theoretical expectations of ~50%.

The width of water and Cr lines at 14.1 T were larger than the values obtained at 9.4 T by a factor of about 1.35, which was

slightly, but markedly less than predicted by de Graaf et al. [4]. The linewidth in the 14.1 T spectra, as fitted by LCModel, was about 11 Hz, which is much smaller than the value of about 14 Hz obtained experimentally on the methyl signal of total Cr at 3.03 ppm. However, the linewidth of the Cr signal comprises not only the natural linewidth but also the difference of 0.002 ppm (1.2 Hz at 14.1 T) between the chemical shifts of PCr and Cr resonances. Its measurement is further likely affected by the overlapping signals of macromolecules, GABA and GSH.

In summary, we conclude that increasing magnetic field strength to 14.1 T improves spectral resolution in *in vivo* ^{1}H NMR spectroscopy, which enables to detect resonances previously not seen in rodent brain. The newly observed spectral features amend the accuracy of metabolite concentrations calculated by LCModel and generally decrease their Cramer–Rao lower bounds.

Acknowledgments

This work was supported in part by the Centre d'Imagerie Bio-Medicale (CIBM) of the UNIL, EPFL, UNIGE, CHUV and HUG, the Leenaards and Jeantet Foundations and by the EU Grant No. MRTN-CT-2006-035801.

References

[1] J. Pfeuffer, I. Tkáč, S.W. Provencher, R. Gruetter, Toward an in vivo neurochemical profile: quantification of 18 metabolites in short-echo-time ^{1}H NMR spectra of the rat brain, J. Magn. Reson. 141 (1999) 104–120.
[2] I. Tkáč, P. Andersen, G. Adriany, H. Merkle, K. Ugurbil, R. Gruetter, In vivo ^{1}H NMR spectroscopy of the human brain at 7 T, Magn. Reson. Med. 46 (2001) 451–456.
[3] V. Mlynárik, S. Gruber, E. Moser, Proton T_1 and T_2 relaxation times of human brain metabolites at 3 Tesla, NMR Biomed. 14 (2001) 325–331.
[4] R.A. de Graaf, P.B. Brown, S. McIntyre, T.W. Nixon, K.L. Behar, D.L. Rothman, High magnetic field water and metabolite proton T_1 and T_2 relaxation in rat brain in vivo, Magn. Reson. Med. 56 (2006) 386–394.
[5] M. Terpstra, P.M. Andersen, R. Gruetter, Localized eddy current compensation using quantitative field mapping, J. Magn. Reson. 131 (1998) 139–143.
[6] R. Gruetter, Automatic, localized in vivo adjustment of all first- and second-order shim coils, Magn. Reson. Med. 29 (1993) 804–811.
[7] I. Tkáč, Z. Starčuk, I.Y. Choi, R. Gruetter, In vivo ^{1}H NMR spectroscopy of rat brain at 1 ms echo time, Magn. Reson. Med. 41 (1999) 649–656.
[8] J. Yang, J. Shen, In vivo evidence for reduced cortical glutamate–glutamine cycling in rats treated with the antidepressant/antipanic drug phenelzine, Neuroscience 135 (2005) 927–937.
[9] J. Yang, J. Shen, Increased oxygen consumption in the somatosensory cortex of alpha-chloralose anesthetized, rats during forepaw stimulation determined using MRS at 11.7 Tesla, Neuroimage 32 (2006) 1317–1325.
[10] K.L. Behar, T. Ogino, Characterization of macromolecule resonances in the ^{1}H NMR spectrum of rat brain, Magn. Reson. Med. 30 (1993) 38–44.
[11] V. Govindaraju, K. Young, A.A. Maudsley, Proton NMR chemical shifts and coupling constants for brain metabolites, NMR Biomed. 13 (2000) 129–153.
[12] A. Naressi, C. Couturier, I. Castang, R. de Beer, D. Graveron-Demilly, Java-based graphical user interface for MRUI, a software package for quantitation of in vivo/medical magnetic resonance spectroscopy signals, Comput. Biol. Med. 31 (2001) 269–286.
[13] S.W. Provencher, Estimation of metabolite concentrations from localized in vivo proton NMR spectra, Magn. Reson. Med. 30 (1993) 672–679.
[14] R. Gruetter, I. Tkáč, Field mapping without reference scan using asymmetric echo-planar techniques, Magn. Reson. Med. 43 (2000) 319–323.
[15] V. Mlynárik, G. Gambarota, H. Frenkel, R. Gruetter, Localized short-echo-time proton MR spectroscopy with full signal-intensity acquisition, Magn. Reson. Med. 56 (2006) 965–970.
[16] R.J. Ordidge, A. Connelly, J.A.B. Lohman, Image-selected invivo spectroscopy (ISIS)—a new technique for spatially selective NMR-spectroscopy, J. Magn. Reson. 66 (1986) 283–294.
[17] C. Geppert, W. Dreher, D. Leibfritz, PRESS-based proton single-voxel spectroscopy and spectroscopic imaging with very short echo times using asymmetric RF pulses, Magn. Reson. Mater. Phy. 16 (2003) 144–148.
[18] R. Mulkern, J. Bowers, Density matrix calculations of AB spectra from multipulse sequences: quantum mechanics meets in vivo spectroscopy, Concepts Magn. Reson. 6 (1994) 1–23.
[19] W.W.F. Pijnappel, A. Van den Boogaart, R. de Beer, D. van Ormondt, SVD-based quantification of magnetic-resonance signals, J. Magn. Reson. 97 (1992) 122–134.
[20] F. Du, X.H. Zhu, H. Qiao, X. Zhang, W. Chen, Efficient in vivo ^{31}P magnetization transfer approach for noninvasively determining multiple kinetic parameters and metabolic fluxes of ATP metabolism in the human brain, Magn. Reson. Med. 57 (2007) 103–114.
[21] A. Lorek, Y. Takei, E.B. Cady, J.S. Wyatt, J. Penrice, A.D. Edwards, D. Peebles, M. Wylezinska, H. Owen-Reece, V. Kirkbride, et al., Delayed (''secondary'') cerebral energy failure after acute hypoxia-ischemia in the newborn piglet: continuous 48-hour studies by phosphorus magnetic resonance spectroscopy, Pediatr. Res. 36 (1994) 699–706.
[22] C. Dautry, F. Vaufrey, E. Brouillet, N. Bizat, P.G. Henry, F. Conde, G. Bloch, P. Hantraye, Early *N*-acetylaspartate depletion is a marker of neuronal dysfunction in rats and primates chronically treated with the mitochondrial toxin 3-nitropropionic acid, J. Cereb. Blood Flow Metab. 20 (2000) 789–799.
[23] G.J. Balcom, R.H. Lenox, J.L. Meyerhoff, Regional γ-aminobutyric acid levels in rat brain determined after microwave fixation, J. Neurochem. 24 (1975) 609–613.
[24] A.M. Mans, M.R. DeJoseph, R.A. Hawkins, Metabolic abnormalities and grade of encephalopathy in acute hepatic failure, J. Neurochem. 63 (1994) 1829–1838.
[25] L. Xin, G. Gambarota, V. Mlynárik, R. Gruetter, Proton T_2 relaxation time of J-coupled cerebral metabolites in rat brain at 9.4 T, NMR Biomed. 21 (2008) 396–401.